

PROPER MOTION OF THE COMPACT, NONTHERMAL RADIO SOURCE IN THE GALACTIC CENTER, SAGITTARIUS A*

D. C. Backer

Astronomy Department & Radio Astronomy Laboratory, University of California, Berkeley, CA
email: dbacker@astro.berkeley.edu

and

R. A. Sramek

Very Large Array, National Radio Astronomy Observatory, Socorro, NM
email: rsramek@aoc.nrao.edu

ABSTRACT

Proper motions and radial velocities of luminous infrared stars in the galactic center have provided strong evidence for a dark mass of $2.5 \times 10^6 M_{\odot}$ in the central 0.05 pc of the galaxy. The leading hypothesis for this mass is a black hole. High angular resolution measurements at radio wavelengths find a compact radio source, Sagittarius (Sgr) A*, that is either the faint glow from a small amount of material accreting onto the hole with low radiative efficiency or a miniature AGN core-jet system.

We provide in this paper a full report on the first program that has measured the apparent proper motion of Sgr A* with respect to background extragalactic reference frame. Our current result is:

$$\mu_{l,*} = [-6.18 \pm 0.19] \text{ mas y}^{-1}$$

$$\mu_{b,*} = [-0.65 \pm 0.17] \text{ mas y}^{-1}.$$

The observations were obtained with the NRAO Very Large Array at 4.9 GHz over sixteen years. The proper motion of Sgr A* provides an estimate of its mass based on equipartition of kinetic energy between the hole and the surrounding stars. The measured motion is largest in galactic longitude. This component of the motion is consistent with the secular parallax that results from the rotation of the solar system about the center, which is a global measure of Oort's constants (A-B), with no additional peculiar motion of Sgr A*. The current uncertainty in Oort's galactic rotation constants limits the use of this component of the proper motion for a mass inference. In latitude we find a small, and weakly significant, peculiar motion of Sgr A*, $-19 \pm 7 \text{ km s}^{-1}$ after correction for the motion of the solar system with respect to the local standard of rest.

We consider sources of peculiar motion of Sgr A* ranging from unstable radio wave propagation through intervening turbulent plasma to the effects of asymmetric masses in the center. These fail to account for a significant peculiar motion. One can appeal to an $m = 1$ dynamical instability that numerical simulations have revealed. However, the measurement of a latitude peculiar proper motion of comparable magnitude and error but with opposite sign in the companion paper by Reid (1999) leads us to conclude at the present time that our errors may be underestimated, and that the actual peculiar motion might therefore be closer to zero.

Improvement of these measurements with further observations and resolving the differences between independent experiments will provide the accuracies of a few km s⁻¹ in both coordinates that will provide both a black hole mass estimate and a definitive determination of Oort's galactic rotation constants on a global galactic scale.

1. INTRODUCTION

The compact, nonthermal radio source, Sgr A*, was discovered by Balick & Brown (1974) while looking for compact HII regions in the center of the galaxy. The nature of Sgr A* and its role in the center of our galaxy have been a matter of speculation over the past 25 years. Until recently theoretical and observational arguments were advanced that the galactic center contains a million solar mass black hole that might be identified with Sgr A* (Lynden-Bell & Rees 1971; Genzel, Hollenbach, & Townes 1994). However, emission across the electromagnetic spectrum definitively identified with, or even possibly identified with, Sgr A* contains no more than 10³⁶ solar luminosities (Beckert et al. 1996; Serabyn et al. 1997) which does not necessarily demand a supermassive object. Angular size measurements of Sgr A* also have yet to reveal definitively the nature of this object owing to the blurring effects of interstellar scattering in the dense, turbulent plasma near the galactic center (Lo et al. 1985; Backer 1988; Jauncey et al. 1989; Frail et al. 1994; Rogers et al. 1994; Bower & Backer 1998; Lo et al. 1998). From the highest frequency VLBI observations we infer an upper limit to the size of 1 AU at 86 GHz (Rogers et al. 1994). Recent summaries of the variability of the radio emission (Zhao et al. 1991; Gwinn et al. 1991; Backer 1994; Wright & Backer 1993; Tsuboi, Miyazaki, & Tsutsumi 1999) and limits on its linear and circular polarization (Zhao 1992, personal communication; Bower & Backer 1999) also do not give us a definitive handle on the intrinsic nature of this object – stellar mass object or supermassive black hole?

Over the past five years our understanding of both the presence of dark matter in the center and the nature of Sgr A* has improved radically. Large proper motions of luminous infrared stars within 0.1 parsec of Sgr A* have now been detected and lead to a good estimate on the central dark mass of $2.5 \times 10^6 M_{\odot}$ (Eckart & Genzel 1997; Genzel et al. 1997; Ghez et al. 1998). However, models for the full Sgr A* electromagnetic flux spectrum based on low radiative efficiency accretion of wind-driven matter from nearby stars onto a black hole are not yet consistent with a

mass of a few million solar masses given nominal estimates of the mass accretion rate (Melia 1992, 1994; Falcke et al. 1993; Falcke & Melia 1997; Narayan, Yi, & Mahadevan 1995; Narayan et al. 1998; Mahadevan 1998).

Shortly after the discovery of Sgr A* we began an astrometry program to determine its proper motion relative to extragalactic reference sources, active galactic nuclei and quasars, with the NRAO ¹ Green Bank interferometer (Backer & Sramek 1982; BS82). If Sgr A* were ‘just’ a stellar mass object, then it would be buzzing around in the central gravitational potential well in equipartition with the other stars and gas clouds in the center. Transverse velocity components of at least 100-200 km s⁻¹ would be expected (Sellgren et al. 1990). Alternatively, if Sgr A* were indeed a supermassive black hole, then it might very well be at rest in the center. Different formation scenarios for such an object as well as considerations of galactic dynamics predict different residual motions of a black hole with respect to the galactic center.

Our observations from the solar system of an object in the galactic center relative to the extragalactic sky are sensitive, of course, to the secular parallax resulting mainly from the rotation of the galaxy with a small additional contribution from the solar motion with respect to the local standard of rest. The expected motion is approximately 6 mas y⁻¹ using current values of galactic constants (Kerr & Lynden-Bell 1986). If we remove this large secular parallax from the apparent motion, the residual, peculiar motion with respect to the galactic barycenter can be used to estimate the mass of Sgr A* using an equipartition or other dynamical argument. The uncertainty in the secular parallax correction is largest in the longitude direction. Therefore, the peculiar motion of Sgr A* in galactic latitude is most important for assessment of mass of the parent body of Sgr A*. Alternatively, if we assume both that Sgr A* is attached rigidly to a several million solar mass black hole and that this object defines the inertial reference frame for the galaxy, then the apparent motion can be used to define galactic constants.

The intensity distribution of Sgr A* is broadened by multipath propagation (diffraction) in the intervening thermal plasma whose density is perturbed on small length scales. The detection of similar broadening of OH masers near Sgr A* by Frail et al. (1994) suggests strongly that this plasma is located in the central 140 pc of the galaxy. The apparent diameter of Sgr A* is 1.4 mas $\lambda^{+2.0}$ where λ is the wavelength in cm. Past and present proper motion measurements have an error much smaller than this size and therefore we have a particular concern about temporal stability of diffractive and refractive propagation effects.

Our Green Bank experiment (1976-1981) detected a proper motion in galactic longitude that was consistent with the expected secular parallax and therefore with negligible peculiar motion or refractive effects (BS82). However the errors were too large to place a meaningful limit on the mass of Sgr A*. They did establish that Sgr A* was galactic and not a chance superposition of an

¹The National Radio Astronomy Observatory is a facility of the National Science Foundation operated under cooperative agreement by Associated Universities, Inc.

extragalactic background source.

In 1981 we began a new Sgr A* proper motion experiment with the NRAO Very Large Array (VLA, see Napier, Thompson, & Ekers 1983). The number of antennas, the two dimensional distribution of antennas in a wye configuration, the excellent site for phase stability and the sensitive receivers provided considerable new capability. Reports of the progress of this experiment have been provided in a series of conference reports (Backer & Sramek 1987; Backer 1994, 1996). In this paper we provide a full report of 8 epochs of VLA observations between 1982 and 1998. The observations are described in §2, and our procedures for the determination of the apparent proper motion of Sgr A* are explained in §3. In §4 we discuss the current best estimate for galactic constants that lead to the $\sim 6 \text{ mas y}^{-1}$ secular parallax in galactic latitude that dominates the measured motion. The possibility of refractive wander of the position of Sgr A* is then explored and limited by recent dual frequency data. The third topic in §4 concerns interpretation of the peculiar motion which remains after subtraction of the estimated secular parallax. A summary of the paper is given in §5.

2. OBSERVATIONS AND DATA REDUCTION

In 1981 we searched the literature for candidate reference sources closer to Sgr A* than those used in the Green Bank experiment reported previously (BS82). The Westerbork planetary nebula searches (Wouterloot & Dekker 1979; Isaacman 1981) provided the most sensitive and highest angular resolution images for location of background quasars or other compact extragalactic sources. We further undertook a blind search at the VLA by making snapshot images at 5 GHz of about 50 fields whose solid angles were determined by a combination of primary and delay beams. The Westerbork candidates were also observed. These efforts led to the identification of 3 reference sources with sufficiently strong fluxes ($>25 \text{ mJy}$) and compact structure ($< 1''$). Sources W56 (B1737-294) and W109 (B1745-291) were from the Westerbork surveys and source GC441 (B1737-294) was the first source cataloged in our 44th blind search beam. Figure 1 provides a map of the sky surrounding Sgr A* with the relative locations of the three reference sources. While these sources are not ‘identified’ as quasars or AGNs, their brightness temperature lower limits and spectra are such that we can confidently assume that they were extragalactic. The three sources yield an estimated source density of 3 per 4 square degrees at an average 5-GHz flux density of 75 mJy. This is consistent with source counts of extragalactic sources (Condon 1984). A test of this primary ‘extragalactic’ assumption is presented in a later section. Table 1 provides the assumed source positions for our primary calibration sources, Sgr A*, and the three reference sources. The initial positions and Besselian 1950 reference frame were assumed for all measurements. In our analysis relative offsets between the three reference sources from their assumed positions were determined. These offsets and the improved positions for all three reference sources are included in Table 1.

There remains a bias in the reference source positions with respect to our primary phase

calibrator, B1748-253, as will be evident when we introduce figure 2. Furthermore our assumed position for B1748-253 at the start of our observations is not accurate as evidenced by hourly observations of the astrometric standard B1741-038. In Table 2 we present J2000 FK5 positions of all sources. The positions of Sgr A* and the three reference sources were kindly provided by G. Bower 1999 during his polarization study. These were referenced to B1748-253 assuming our original coordinates. The four positions were then corrected for the errors in the original B1748-253 coordinates as determined by that listed in the current VLA manual and that determined in our data via the B1741-038 observations. Our estimate of the 1σ absolute accuracy is 5 mas.

From 1982 to 1998 a sequence of eight observations at 4.885 GHz were conducted using the VLA in its 36-km (A) configuration. In more recent epochs a second band was recorded at 4.835 GHz, but this data was typically not analyzed owing to the dominance of atmospheric errors that are very strongly correlated between the two bands. In the last three epochs a portion of the standard observing schedule was devoted to observations at 8.435 GHz and 8.485 GHz. Typically three days of observations were obtained each epoch. In the text below we refer to the two bands by their center frequencies of 4.9 and 8.4 GHz

Each day’s observations were divided into hour-long blocks. During each block we first observed the 3 nearby reference sources, then Sgr A*, then 2 reference sources, then Sgr A*, then 2 reference sources, etc, with a final observation of the 3 reference sources. Every hour our phase calibration source B1748-253 and a standard VLA calibration source B1741-038 were observed. Table 3 gives a detailed UT schedule for a block to show typical integration times and spacings. Identical LST stop times were used to schedule all observations. Sgr A* was observed every 10 minutes in these blocks. During epochs 6 through 8 we allocated one LST block to 8.4-GHz observations. Given that our analysis had shown that the dominant errors in phase referencing were temporal rather than angular we revised the schedule for the 8.4-GHz observations by looking at only one reference source between Sgr A* scans and therefore returning to Sgr A* every 6 minutes.

Table 4 provides a journal of the observations with epoch number, sequential day index within the epoch, calendar date, Julian Date and a code to indicate which band was observed during which block (C for 4.9 GHz and X for 8.4 GHz). LST blocks at 15, 16, 17, 18 and 19 h were originally used with all observations at 4.9 GHz. In later epochs we observed at 8.4 GHz during 18h block and dropped the 15h block. For recovery of the files containing these observations we include in Table 4 information needed to access the archive tapes at NRAO in Socorro, NM.

Calibration proceeded along standard lines for the VLA. The flux densities for 3C 286 were established with the SETJY task. Then the CALIB task was run to determine the gains for 3C 286 using recommended UV restrictions. Next CALIB was run on secondary flux standards: B1748-253, B1741-038, 3C 48, and NRAO 530. The flux densities of these sources were determined using the GETJY task. The program source, Sgr A* and the 3 reference sources, were then calibrated in flux and phase using two-point interpolation of the B1748-253 data via the CLCAL

task. These calibration steps are described using the current AIPS program names while the earliest epochs of data were processed using predecessor versions of the software. The hourly calibration to B1748-253 removed instrumental phases and part of the atmospheric phase. While this helps in subsequent data analysis, the effects of this phase calibration are accurately removed by the reference source comparison described below. For epochs 1-7 this initial stage of data reduction was done at NRAO facilities in Datil or Socorro. For the last epoch reduction was done in Berkeley.

Our main approach to the analysis of each source observation uses the 351 complex visibility phases for each orthogonally polarized channel along with the time of the observation and a table of antenna positions. These were created within the VLA DEC10 and AIPS analysis systems by directing a matrix of scan and vector averaged phases to a disk file using the LISTER task. This procedure was easy to replicate each epoch as the VLA developed, and allowed us freedom to develop algorithms for precise phase referencing. Recently we reanalysed raw data from epochs 2 and 4 to ensure that there are no systematic errors in these matrix listings of phases as well as the associated times, positions and antenna locations. We conclude that there are no systematic effects at the milliarcsecond level in the second difference position offsets described below.

3. ANALYSIS

The phase calibration described in §2 using B1748-253 every hour leaves as much as one radian of residual phase on the longer baselines with time scales for variation as fast as 15 minutes. We reason that the bulk of this differential atmospheric phase can be modeled by a differential refraction angle, which is differential owing to the B1748-253 calibration. In other words, the phases for any scan can be modeled by a plane wave deviation from the assumed source direction. Furthermore we expect that the differential refraction angles for our three reference sources will differ from those of Sgr A* according to a simple Taylor series expansion in angle on the sky and in time. The discussion focuses here on atmospheric perturbations (*i.e.*, tropospheric and ionospheric), but any source of astrometric error (*e.g.*, frequency, time, baseline, reference frame) will have similar effects. While previous experience and analysis supported this approach, we know that the differential phase fluctuations from the atmosphere will show higher order spatial variations than the plane-wave assumption in this model. We expect, however, that the effects of these higher order terms will be similarly encoded in the differential refraction angles for the set of sources.

Our first program reads a scan of phases and associated antenna locations, and then fits them to a plane wave model to produce the instantaneous refraction angle, $\Delta\mathbf{s}_i(t_j)$ with an iteration algorithm. Sidereal time is calculated from the recorded TAI values, and current coordinates of the sources were rotated from the B1950.0 positions (Table 1). On the first iteration only phase data from baselines with projected lengths between 150 and 200 $k\lambda$ are used. The minimum excludes baselines for which large scale structure will confuse the phase. The maximum prevents use of

data that may have a 2π lobe ambiguity. Phases that exceed 90° are excluded owing to a possible lobe ambiguity. On the next iteration, the first estimate is used and the maximum baseline is extended to include the full array. One final pass is done to insure that the maximum amount of data is used. Each $\Delta\mathbf{s}_j$ solution has its internal error estimated from the variations of the phases. Much of the phase variation is not independent from baseline to baseline, so this internal error estimate will underestimate the uncertainty. The error will however reflect the phase scatter, and so is useful as a relative weight in further analysis.

Figure 2 displays three sets of these differential refraction angles for one day each in epochs 2, 3 and 8. The data from epochs 2 and 8 show the best differential phase stability. In general, the four sources, Sgr A* and the three reference objects, meander back and forth with an amplitude of $0.1''$ on a time scale of one half hour. The data from epoch 3 (1983 September 2) display the worst differential phase stability in the entire experiment.

One can readily see in Figure 2 that the position of Sgr A* drifts away from the cluster of reference sources over the sixteen year span of the data in both right ascension and declination which corresponds to an apparent motion toward negative galactic longitude. This drift is caused mainly by the inexorable rotation of the solar system around the center of the galaxy!

In our next analysis step we interpolate the differential refraction angles of the reference source observations to the times and position of the Sgr A* observations. Figure 2 demonstrates that temporal variations dominate. If we were to start the program over, we would choose to switch sources even more rapidly. We separately analyse the data within each of the one hour blocks of the schedule. Position offsets are removed from the reference sources as we have used constant source position models for all observations, while we determined improved positions in later years. All reference source data in a given block, typically 12 observations, are fit to an 8th order polynomial in time. This polynomial is then evaluated at the times of all sources and removed. Then a simple two-point calibration is done between the data of all reference sources for each Sgr A* observation. Examples of these polynomials are shown in Figure 2.

These two analysis steps can be represented as follows: First the χ^2 sums are defined that allow solution for the right ascension (a_k) and declination (d_k) polynomial coefficients.

$$\chi_a^2 = \sum_{i=1,3} [\Delta\alpha_i(t_j) - \sum_{k=0}^{k=n} a_k(t_j - \langle t \rangle)^k]^2. \quad (1a)$$

$$\chi_d^2 = \sum_{i=1,3} [\Delta\delta_i(t_j) - \sum_{k=0}^{k=n} d_k(t_j - \langle t \rangle)^k]^2. \quad (1b)$$

Then the polynomial coefficient estimates (\hat{a}_k, \hat{d}_k) are used to remove this effect from all sources.

$$\Delta\alpha'_i(t_j) = \Delta\alpha_i - \sum_{k=0}^{k=n} \hat{a}_k(t_j - \langle t \rangle)^k. \quad (2a)$$

$$\Delta\delta'_i(t_j) = \Delta\delta_i - \sum_{k=0}^{k=n} \hat{d}_k (t_j - \langle t \rangle)^k. \quad (2b)$$

Finally the primed reference source data are interpolated in time, combined with weights to effect an interpolation in angle, and subtracted from the primed Sgr A* data.

$$\Delta s''_*(t_j) = \Delta s'_*(t_j) - \sum_{i=1}^{i=3} w_i \left[\Delta s'_i(t_{j+}) \left(\frac{t_j - t_{j-}}{t_{j+} - t_{j-}} \right) + \Delta s'_i(t_{j-}) \left(\frac{t_{j+} - t_j}{t_{j+} - t_{j-}} \right) \right]. \quad (3)$$

The optimal weights were chosen such that the mean weighted reference position was equal to that of Sgr A*: 0.288, 0.288, and 0.424 for GC441, W56, and W109, respectively. One can estimate these weights by inspection of Figure 1 which has the right ascension of W56 nearly equal to that of Sgr A* and the declination of W109 nearly that of Sgr A*, and the right ascension offset of GC441 nearly double and opposite that of W109 and the declination of GC441 nearly equal and opposite that of W56. The errors are propagated from the internal errors carried along with the various steps outlined above. In the best conditions these errors do indicate the agreement of the data. The errors also display when the data is less good, but as stated earlier, the magnitude of the errors may underestimate the expected data agreement owing to correlation of phase errors between baselines.

Our next step is to combine the position offsets for Sgr A* for each block on each day using the internally propagated errors as weighting factors. The poor quality of the low elevation data in the 15h LST block leads us to ignore this data for all days. Only on a few occasions does its quality match that of the higher elevation data. The results of this block averaging for the 4.9-GHz data are displayed in Figure 3 along with a weighted least squares fit for a proper motion which is:

$$\mu_{\alpha,*} = -2.70 \pm 0.15 \text{ mas y}^{-1}. \quad (4a)$$

$$\mu_{\delta,*} = -5.60 \pm 0.20 \text{ mas y}^{-1}. \quad (4b)$$

This fit is presented in Figure 4 along with the results of six other fits to subsets of the data. In three subsets we selected one of the three days in each epoch. In the other three subsets we selected one of the three hour angle blocks which are available for all epochs. These provide a measure of the effects of the troposphere and other errors on our measurement and serve as our primary estimator of uncertainty in the measured proper motion. We also explored the chance possibility that the reference sources themselves might be galactic by setting the weight of each reference source to 0 in separate runs. The results are all contained in the error polygon shown in Figure 4 which is used to estimate the errors quoted above. We conclude then that the reference sources are indeed extragalactic and not chance compact objects in the center themselves.

The 3-epoch, 8.4-GHz data also provided a proper motion fit which is presented in Figure 4. The result is consistent with the 4.9-GHz result quoted above although the errors are larger. Again we used the data on independent days to provide three independent fits to assess errors.

The phase analysis discussed here has been done primarily on computers at Berkeley with migration from VAX to μ VAX to SUN.

Use of the B1950 coordinate frame is not ideal for precision astrometry owing to improved precession constants and its incorporation of E-terms of aberration into the calibrator source positions. However, our differential technique suppresses errors in the reference frame and calculation of apparent coordinates for use in observation time modeling of the fringe phase. We have inspected the effects of the B1950 system by precessing source positions at and near Sgr A* from 1950 to various epochs in the range of 1981 to 1998 with old precession and nutation values and then to 2000 using the new values as specified for FK4 to FK5 catalog conversions by Seidelman (1992; §3.5). We find that a false proper motion of

$$\delta\mu_\alpha = -0.0 \text{ mas y}^{-1}. \quad (5a)$$

$$\delta\mu_\delta = -0.2 \text{ mas y}^{-1}. \quad (5b)$$

is induced. This small motion is similar for our three reference sources and therefore has negligible effect on our measurements. The size of the effect is significantly larger in other parts of the sky.

4. INTERPRETATION

4.1. Secular parallax for object at rest in the galactic center

The expected motion for an object at rest in the galactic barycenter, its secular parallax, is given in galactic coordinates by

$$[\mu_l, \mu_b]_\Pi = [\mu_l, \mu_b]_{\text{GR}} + [\mu_l, \mu_b]_\odot = -[(A - B), 0] - [V_\odot/R_\odot, W_\odot/R_\odot], \quad (6)$$

where A and B are Oort's constants expressed in angular terms, V_\odot and W_\odot give the solar motion with respect to the local standard of rest in directions of $l = 90^\circ$ and $b = 90^\circ$, respectively, and R_\odot is the distance to the galactic center. The 1984 IAU adopted value for $(A - B)$ is $26.4 \pm 1.9 \text{ km s}^{-1} \text{ kpc}^{-1}$ (Kerr & Lynden-Bell 1986). More recent determinations are consistent with this value: (Hanson 1987) uses the Lick northern sky proper motion data to obtain $25.2 \pm 1.9 \text{ km s}^{-1} \text{ kpc}^{-1}$; Feast & Whitelock (1997) use of a Hipparcos study of cepheid stars yields $27.2 \pm 1.0 \text{ km s}^{-1} \text{ kpc}^{-1}$; Olling & Merrifield (1998) use a more complete model of the galactic mass field to determine $25.2 \pm 1.9 \text{ km s}^{-1} \text{ kpc}^{-1}$; and Feast, Pont, & Whitelock (1998) analyze cepheid period-luminosity zero point from radial velocities and Hipparcos proper motions and revise their previous result to $27.23 \pm 0.86 \text{ km s}^{-1} \text{ kpc}^{-1}$. As the 1984 IAU value of $(A - B)$ remains in the midst of these new estimates we will use this in further calculations.

$$[\mu_l, \mu_b]_{\text{GR}} = [-5.57 \pm 0.42, 0.0] \text{ mas y}^{-1}. \quad (7)$$

The solar motion has been determined by Dehnen & Binney (1998) using Hipparcos results: $(U_\odot, V_\odot, W_\odot) = (11.0 \pm 0.4, 5.3 \pm 0.6, 7.0 \pm 0.4) \text{ km s}^{-1}$. The apparent proper motion owing to

solar motion with respect to the local standard of rest using $R_{\odot} = 8.5$ kpc is

$$[\mu_l, \mu_b]_{\odot} = [-0.13 \pm 0.02, -0.17 \pm 0.01] \text{ mas y}^{-1}. \quad (8)$$

The total secular parallax is

$$[\mu_l, \mu_b]_{\Pi} = [-5.70 \pm 0.42, -0.17 \pm 0.01] \text{ mas y}^{-1}. \quad (9)$$

The solar motion contributes negligible additional uncertainty to the secular parallax.

4.2. Apparent peculiar motion of Sgr A*

We project the observed proper motion, equation 4, from equatorial coordinates to galactic coordinates and remove the expected secular parallax for an object at rest in the galactic barycenter, equation 9, to obtain the peculiar motion. The north celestial pole (NCP), north galactic pole (NGP), and galactic center (GC) form a spherical triangle. The equatorial coordinates of the NGP and the GC are: $12^h 49^m$ and $+27^{\circ} 24'$; and $17^h 42^m 24^s$ and $-28^{\circ} 55'$, respectively (B1950; Blaauw et al. 1960). The spherical angle NGP-NCP-GC is then 73.37° and the side of the triangle opposite NGP-GC-NCP has length 62.60° . NGP-GC-NCP is the negative of the position angle ² of the positive galactic latitude axis (\hat{b}), and by law of sines is -58.29° . The position angle of the positive longitude axis (\hat{l}) is then $+31.71^{\circ}$. Errors in determination of the galactic pole and center are of order $7'$ (Blaauw et al. 1960) and hence of little consequence to these calculations. Redetermination of the principal plane of the galaxy via population II stars seen by IRAS (Habing 1988) would be an interesting stellar mass check on the early HI gaseous disk determination. The resultant observed proper motion of Sgr A* in galactic coordinates is

$$\mu_{l,*} = [-6.18 \pm 0.19] \text{ mas y}^{-1} \quad (11a)$$

$$\mu_{b,*} = [-0.65 \pm 0.17] \text{ mas y}^{-1} \quad (11b).$$

The observed peculiar motion of Sgr A* is then obtained by subtracting the expected secular parallax, equation 9, from the measurements:

$$\Delta\mu_{l,*} = [-0.48 \pm 0.46] \text{ mas y}^{-1} \quad (12a)$$

$$\Delta\mu_{b,*} = [-0.48 \pm 0.17] \text{ mas y}^{-1} \quad (12b).$$

The errors have been combined in quadrature. At a distance of 8.5 kpc the peculiar velocity of Sgr A* is

$$v_{l,*} = [-19 \pm 19] \text{ km s}^{-1} \quad (13a)$$

$$v_{b,*} = [-19 \pm 7] \text{ km s}^{-1} \quad (13b).$$

In the subsequent sections we discuss this result further.

²position angles are measured north toward east, counterclockwise on the sky

4.3. Radio wave propagation effects

VLBI observations show that the apparent angular diameter of Sgr A* depends strongly on frequency, $1.4 \text{ mas } \lambda^{+2.0}$, which is consistent with angular broadening by scattering in the intervening plasma (Lo et al. 1981, 1985; Backer 1988; Jauncey et al. 1989; Lo et al. 1993; Alberdi et al. 1993; Yusef-Zadeh et al. 1994; Backer 1994; Rogers et al. 1994; Bower & Backer 1998; Lo et al. 1998). The scattering interpretation is strengthened by the demonstration that OH masers within 0.5 degrees of Sgr A* are similarly broadened (van Langevelde et al. 1992; Frail et al. 1994). A simple explanation is that the diffuse thermal plasma in the central 140 pc (diameter in longitude) is sufficiently turbulent to produce the observed scattering. This gas may be that seen in long wavelength thermal bremsstrahlung emission by Mezger & Pauls (1979) which has an emission measure of at least $10^4 \text{ cm}^{-6} \text{ pc}$. Alternatively there may be scattering within material that is being accreted onto the black hole and serves as fuel for Sgr A* (Backer & Sramek 1999); see also §5 of van Bueren (1978), a comprehensive ‘pre-ADAF’ explanation of Sgr A* as an accreting black hole.

While most of these observations have been conducted in the northern hemisphere where VLBI baseline coverage is poor, several experiments have shown convincingly that the scatter-broadened image is elliptical with a ratio of axes of about 2:1 at position angle (PA) $\sim 80^\circ$. The strong ellipticity in scattering most likely indicates that the scattering gas is threaded by a relatively uniform magnetic field whose pressure dominates the thermal and turbulent pressures of the plasma. The thin ‘threads’ of synchrotron emission detected in the galactic center provide ample evidence for strong and uniform magnetic fields (Yusef-Zadeh, Morris, & Chance 1984). The field is not uniform over scales of 50 pc as the OH maser elongations are not aligned.

Our concern here is not so much with the scattering itself, but rather with the *stability* of the scattering. Consider a scattering screen located a distance fD from Sgr A* with the observer at D . The screen broadens a plane wave by an angle Θ_s . The observed source size is then $\theta_o = f\Theta_s$ which leads to a decorrelation in the visibility domain on baselines of length $b_o = 1/(2\pi f\Theta_s)$. This decorrelation arises from phase differences through the screen on length scales of fb_o . For 4.9 (8.4) GHz this is $240f$ ($400f$) km. The identification of the scattering with a 140-pc halo around the galactic center suggests $f \simeq 0.01$ and therefore decorrelation on extremely small scales, 2.4 (4.0) km. These length scales are most likely smaller than the inner scale of the density fluctuation spectrum which is set by plasma wave dissipation processes. When phase decorrelation occurs on scales much smaller than that of the density fluctuations owing to many radian phase wrapping, the expected dependence of scattering diameter on wavelength is exactly $\lambda^{+2.0}$ which is consistent with current observations. In this regime we also don’t expect image wander from large scale refractive effects, and any changes in the angular broadening will occur on long time scales set by θ_o/v_\perp where v_\perp is the transverse motion of the line of sight through the perturbing plasma. We proceed to inspect the evidence for stable propagation through the intervening medium.

The relevance of this discussion to our proper motion measurements is that our epoch accuracy

is around 1-2 mas while the scatter broadened image is 50 (18) mas (and VLA synthesized beam is 500 (180) mas) at 4.9 (8.4) GHz, respectively. The scattered image size itself is very stable. Lo et al. (1981) determined a size at 8.4 GHz of 17 ± 1 mas in 1974.4 with principal resolution in the East-West direction. Later measurements in 1983.4 had sufficient UV coverage to determine elliptical source parameters: 15.5 ± 0.1 mas with axial ratio of 0.55 ± 0.25 and PA of $98^\circ \pm 15^\circ$ (Lo et al. 1985). Recent VLBA observations provide parameters of 18.0 ± 1.5 mas with ratio of 0.55 ± 0.14 and PA of $78^\circ \pm 6^\circ$ (Lo et al. 1998). We conclude that the source size has not changed by more than 5-10% over 23 y either with random or secular variations. Thus the apparent source image is not expanding or contracting at a rate any larger than 0.07 mas y^{-1} at 8.4 GHz.

The time scale for the scattered image to sample an independent portion of the turbulent screen is given by the ratio of the linear size of the image to the velocity of the screen relative to the line of sight. If we take this transverse velocity to be 100 km s^{-1} , which is characteristic of the rotating molecular disk, then independent samples of any refractive beam wander (or source size change) will occur on time intervals of 20 (7) years, respectively. Over the somewhat shorter 16-y interval of our 4.9-GHz measurements, we might see just a linear change of the position if our above conclusion that refraction was not important was wrong. The typical contribution to the proper motion from refractive wander is $0.25g \text{ mas y}^{-1}$, where $g(t)$ is the fractional shift of the centroid of the scattering disk from its long term average. Statistically the amplitude of this false motion would be frequency independent as the time scale shortens with frequency just in proportion to the apparent size. During any short time interval the refractive motion will differ over an octave of frequency, and so we could expect that the effects at our two radio frequencies would differ.

A separate test of refractive effects is to look at the differential positions at the two frequencies at a single epoch. In our Green Bank experiment (BS82) we found that the differential positions at 2.7 and 8.1 GHz were identical to within ~ 0.02 of the scattering diameter at 2.7 GHz. Note that the reference sources in the Green Bank and VLA experiments differ. In Figure 5 we show the differential Sgr A* positions from three days of observations in epoch 8 at 4.9 GHz and 8.4 GHz. There is a systematic offset of ~ 5 mas in right ascension which is 0.1 times the scattering diameter at 5 GHz. Source structure can be one source of difference although 5 mas is large value for this effect. Without further high resolution imaging and monitoring we cannot determine the source or the stability of this offset. A similar offset is seen in the epoch 7 data although the errors are somewhat larger. We conclude that even if refractive wander is present, g is no more than 0.1 and the apparent motion it might contribute is less than our current errors.

4.4. Dynamical effects on the central black hole

A black hole in the center of the galaxy will have a statistical motion with respect to the galactic barycenter owing to the influence of the uneven momentum distribution of objects surrounding it. Consider the motion induced by the transit, or orbit, of a perturbing mass (m_2)

such as a nearby star or a passing molecular cloud. The affect of m_2 on the mass enclosed ($m_1(r)$), and therefore Sgr A*, is given by the acceleration Gm_2/r^2 acting for a time given by r divided by the circular velocity at r , $r/v_c(r)$. The circular velocity at r is given by $\sqrt{Gm_1(r)/r}$. The resulting motion of the barycenter (towards m_2) is then:

$$\Delta v_{\text{BC}} = \frac{\sqrt{G}m_2}{\sqrt{rm_1(r)}}. \quad (14)$$

Figure 6 shows the mass and radial distance of a number of asymmetric masses in the center of the galaxy. In general these appear to grow as $r^{\sim 1.5}$ which is shown in the Figure 6. The asymmetric masses range from the nearest solar mass star whose orbital period is long with respect to our measurement interval to the star formation complex, Sgr B2. Inside of about 1 pc m_1 is constant as shown by the IR stellar motions (Eckart & Genzel 1997; Ghez et al. 1998) and Δv_{BC} will be proportional to r as one considers various contributions to the barycentric motion. The resultant motions, however, are small, less than 1 km s^{-1} . In the range of 1 pc to 100 pc the enclosed luminous mass grows as $r^{1.2}$ based on 2- μm measurements (see review by Genzel et al. (1994)). Mass asymmetries in this range then have an influence on the barycenter motion that grows more slowly as $r^{0.4}$. For example, the molecular cloud M-0.02-0.07 shown in Figure 6 will give the enclosed mass at its radius a peculiar motion of about 1 km s^{-1} . As one goes to larger and larger radii the peculiar motion from mass asymmetries will be increasingly dominated by a longitude motion and not a latitude motion which is the central concern in this paper. We conclude that the influence of mass asymmetries in the galactic center can be ignored at the present level of accuracy.

The perturbations of few km s^{-1} that are expected for a central black hole in our galaxy based on the discussion above can be compared to that expected in other galaxies based on observed asymmetries. The nature of the double nucleus in M31 remains uncertain. The nucleus has probably been identified by the large velocity dispersion at the location of the P2 nucleus (Statler et al. 1999). The other nucleus, P1, may be a concentration of stars in an eccentric disk (Tremaine 1995). Alternatively P1 may be a star cluster which will shortly be ‘absorbed’ into the central by tidal disruption. In either case the observations indicate that the $7 \times 10^7 M_{\odot}$ black hole and the surrounding stars will not be at rest in the mass center of M31 at the level of 10 km s^{-1} owing to the influence of the estimated $3 \times 10^6 M_{\odot}$ stars in P1. This mass asymmetry in M31 is considerably larger than that known for our galaxy at a comparable radius (Fig. 6).

One source of the excitation of an eccentric disk in M31 mentioned above is an unstable $m = 1$ normal mode in an axisymmetric disk. Numerical N-body simulations by Miller & Smith (1992) have shown that the core of galaxies will exhibit motions owing to an unstable $m = 1$ normal mode of oscillation. For the parameters of our galactic center the black hole and its associated cusp of stars could be moving as fast as 70 km s^{-1} (Miller 1996). The instability is the result of an amplification of the small motions discussed above. The direction of this putative motion is arbitrary if the perturbations are the result of mass asymmetries on scales less than 100 pc. Over these scales there is as much evidence for order as disorder with respect the well defined galactic

plance seen on kpc scales. At the level of 70 km s^{-1} we definitely don't see the effect predicted by Miller. We can be unlucky and the motion may be largely radial. If so, we would expect the black hole to be offset in angle from the centroid of stars at larger radii which could be tested with analysis of the IR stellar distribution.

If there is a massive black hole at the center of the galaxy, Gould & Ramirez (1998) have shown that our limit on the observed acceleration implies that Sgr A* is either coincident with or closely bound to that black hole. They point out that acceleration has the advantage of not being confused by uncertainty in Oort's constants. If one expresses both the peculiar velocity and the acceleration of Sgr A* in units of the Earth's motion around the Sun, the normalized velocity and acceleration are equal at a distance of 140 AU for a gravitational mass of $2.5 \times 10^6 M_{\odot}$. Acceleration measurements, or limits, are therefore relatively more important for distances inside 140 AU if the measurements have comparable precision in Earth units. If Sgr A* is a random object in the gravitational potential that one can establish firmly from the IR proper motion studies, then its acceleration is expected to be $0.27 a_{\oplus}$, where a_{\oplus} is the acceleration of the Earth in its orbit around the sun. Our upper limit of the acceleration allowed using the full 1982 to 1998 data set is 0.3 mas y^{-2} , or $0.06 a_{\oplus}$. This result, although slightly higher than that used by Gould & Ramirez is still a small compared to that of a low mass object near the massive black hole. By comparison, the precision of our latitude peculiar motion is 7 km s^{-1} , or $0.21 v_{\oplus}$. We conclude that If the center harbors a massive black hole, then the radio source Sgr A* must be attached to it. They also discuss the possibility that Sgr A* is in very close orbit around the black hole with an excursion less than our single epoch precision and orbital period less than our time base. The VLBA result of Reid (1999) and its comparison with the longer duration VLA result here will place further constraints on this extreme scenario.

Gould & Ramirez also use the limit on acceleration to state the low probability of Sgr A* being a random object passing through a dense cluster of weakly interacting dark matter. In their conclusion they return to this scenario and describe a test using flux density variations caused by Doppler boosting. Such variations would be evident in the daily sampled data discussed by Backer (1994). They note in passing that the equipartition mass of Sgr A* based on the acceleration limit is $250 M_{\odot}$ based on a $10 M_{\odot}$ characteristic mass. The 'equipartition' mass limit for Sgr A* based on the limit on peculiar motion of $< 19 \text{ km s}^{-1}$ and $10 M_{\odot}$ IR stars moving at 1000 km s^{-1} is $> 2 \times 10^4 M_{\odot}$.

Maoz (1998) discusses the dynamical constraints on alternatives to supermassive black holes in galactic nuclei. Critical to his discussion are estimates of the black hole mass and surrounding density in the cusp of stars that form around the black hole. Sgr A*'s diameter upper limit from the 3mm VLBI measurements of Rogers et al. (1994) is 1 AU. When combined with the mass limit this leads to a lower limit for its density of $\sim 10^{21} M_{\odot} \text{ pc}^{-3}$. As noted by Maoz (1998 personal communication), one can argue this point. The radio emission may come from the *central* body of a cluster or a disk and hence may not delimit the full size of the parent mass. In proceeding we assume that the radio emission encompasses the parent mass as it would in the

case of quasi-spherical accretion and core-jet models. The density estimate is such that any form of matter other than a black hole will have a dissipative lifetime less than 10^8 y.

5. CONCLUSION

Measurements with the NRAO Very Large Array from 1982 to 1998 at 4.8 GHz have provided the first proper motion of the compact radio source in our galactic center, Sgr A*. The peculiar motion of Sgr A* in the mass center of the galaxy is obtained after removing an estimate of the secular parallax which results from the solar motion. In latitude the estimated peculiar motion is 19 ± 7 km s⁻¹. Our ongoing uncertainty about the nature of Sgr A* leads us to use the limit on peculiar motion along with an equipartition argument to place a lower bound on its mass of $2 \times 10^4 M_\odot$. The inferred mass density of Sgr A* is then $10^{21} M_\odot \text{pc}^{-3}$ based on a previous estimated 1 AU source diameter at 86 GHz. This is the highest mass density inferred for any galactic black hole candidate. Mass density is currently the best argument for existence of a black hole when consideration is given to the stability of configurations of dark matter other than a solitary black hole.

The simplest model is that Sgr A* is radiation from the atmosphere of the $2.5 \times 10^6 M_\odot$ black hole. Nearly steady infall and outflow models for the radiative properties of Sgr A* exist. The possibility of a non-zero peculiar motion has led to consideration of the influence of known mass asymmetries in the central region of our galaxy. We conclude that these would account for no more than a few km s⁻¹ perturbation. Another source of motion may be a $m = 1$ instability in the central potential. Our estimated peculiar motion is in fact smaller than the estimated size of this effect although projection factors need to be considered to make a firm statistical statement.

A nonzero proper motion might be attributed to systematic errors in the measurements, time variable frequency dependent effects, or variations in the intrinsic structure. At 4.8 GHz Sgr A* is scattered by angles significantly greater than our relative position measurement accuracy. While one can argue that variable refraction is probably not important, this remains a source of uncertainty for the VLA measurements. Models for the radio emission of Sgr A* suggest an increasing intrinsic source size with decreasing radio frequency. This could lead to additional systematic effects for the VLA measurements. Further measurements at higher radio frequencies are planned to resolve these uncertainties.

We commend the National Radio Astronomy Observatory and its staff for developing and maintaining the superb Very Large Array instrument and for providing ample support during this extended observing campaign. The genesis of the VLA experiment started with the 1976-1981 Green Bank experiment, and that was inspired by a lunch time conversation with R. Fisher in Green Bank circa 1975. The authors support has been from UC Berkeley, NAIC, and NRAO and we therefore thank the NSF and California taxpayers. We thank M. Reid for discussions about his

and our measurements, and E. Maoz, A. Sternberg and I. King for comments on the manuscript. G. Bower provided a valuable independent analysis of absolute positions from the epoch 8 data set.

REFERENCES

- Alberdi, A., Lara, L., Marcaide, J. M., et al. 1993, *A&A*, 277, L1
- Backer, D. C. 1988, *AIP Conf. Proc.*, 174, 111
- . 1994, *NATO ASI*, C 445, 403
- Backer, D. C. 1996, in proceedings of IAU Symposium 160 ([Reidel : Dordrecht]), 193
- Backer, D. C. & Sramek, R. A. 1982, *ApJ*, 260, 512
- . 1987, *AIP CP*, 155, 163
- Backer, D. C. & Sramek, R. A. 1999, in *Galactic Center Workshop 98: The Central Parsecs* ([000 : 000]), in press
- Balick, B. & Brown, R. L. 1974, *ApJ*, 194, 265
- Beckert, T., Duschl, W. J., Mezger, P. G., et al. 1996, *A&A*, 307, 450
- Blaauw, A., Gum, C. S., Pawsey, J. L., et al. 1960, *MNRAS*, 121, 123
- Bower, G. C. & Backer, D. C. 1998, *ApJ*, 496, L97
- Bower, G. C. & Backer, D. C. 1999, in *Galactic Center Workshop 98: The Central Parsecs*, ed. H. Falcke ([000 : 000]), in press
- Bower, G. C., Backer, D. C., Zhao, J.-H., et al. 1999, *ApJ*, 00, 00
- Condon, J. J. 1984, *ApJ*, 287, 461
- Dehnen, W. & Binney, J. J. 1998, *MNRAS*, 298, 387
- Eckart, A. & Genzel, R. 1997, *MNRAS*, 284, 576
- Falcke, H., Biermann, P. L., Duschl, W. J., et al. 1993, *A&A*, 270, 102
- Falcke, H. & Melia, F. 1997, *ApJ*, 479, 740
- Feast, M., Pont, F., & Whitelock, P. 1998, *MNRAS*, 298, L43
- Feast, M. & Whitelock, P. 1997, *MNRAS*, 291, 683
- Frail, D. A., Diamond, P. J., Cordes, J. M., et al. 1994, *ApJ*, 427, L43
- Genzel, R., Eckart, A., Ott, T., et al. 1997, *MNRAS*, 291, 219
- Genzel, R., Hollenbach, D., & Townes, C. H. 1994, *Rep. on Prog. in Physics*, 57, 417

- Ghez, A., Klein, B. L., Morris, M., et al. 1998, *ApJ*, 509, 678
- Gould, A. & Ramirez, S. V. 1998, *ApJ*, 497, 713
- Gwinn, C. R., Danen, R. M., Middleditch, J., et al. 1991, *ApJ*, 381, L43
- Habing, H. J. 1988, *A&A*, 200, 40
- Hanson, R. B. 1987, *AJ*, 94, 409
- Isaacman, R. 1981, *A&A Suppl.*, 43, 405
- Jauncey, D. L., Tzioumis, A. K., Preston, R. A., et al. 1989, *AJ*, 98, 44
- Kerr, F. J. & Lynden-Bell, D. 1986, *MNRAS*, 221, 1023
- Lo, K. Y., Backer, D. C., Ekers, R. D., et al. 1985, *Nature*, 315, 124
- Lo, K. Y., Backer, D. C., Kellermann, K. I., et al. 1993, *Nature*, 362, 38
- Lo, K. Y., Cohen, M. H., Readhead, A. S. C., et al. 1981, *ApJ*, 249, 504
- Lo, K. Y., Shen, Z.-Q., Zhao, J.-H., et al. 1998, *ApJ*, 508, L61
- Lynden-Bell, D. & Rees, M. J. 1971, *MNRAS*, 152, 461
- Mahadevan, R. 1998, *Nature*, 394, 651
- Maoz, E. 1998, *ApJ*, 494, L181
- Melia, F. 1992, *ApJ*, 387, L25
- . 1994, *ApJ*, 426, 577
- Mezger, P. G. & Pauls, T. 1979, in *IAU Symp. 84*, ed. W. B. Burton ([Reidel : Dordrecht]), 357
- Miller, R. H. 1996, *ASP CS*, 102, 327
- Miller, R. H. & Smith, B. F. 1992, *ApJ*, 393, 508
- Napier, P. J., Thompson, A. R., & Ekers, R. D. 1983, *Proc. IEEE*, 71, 1295
- Narayan, R., Mahadevan, R., Grindlay, J. E., et al. 1998, *ApJ*, 492, 554
- Narayan, R., Yi, I., & Mahadevan, R. 1995, *Nature*, 374, 623
- Olling, R. P. & Merrifield, M. R. 1998, *MNRAS*, 295, 737
- Reid, M. J. 1999, *ApJ*
- Rogers, A. E. E., Doeleman, S., Wright, M. C. H., et al. 1994, *ApJ*, 434, L59

- Seidelman, P. K. 1992, Explanatory Supplement of the Astronomical Almanac ([University Science : Mill Valley])
- Sellgren, K., McGinn, M. T., Becklin, E. E., et al. 1990, ApJ, 359, 112
- Serabyn, E., Carlstrom, J., Lay, O., et al. 1997, ApJ, 490, L77
- Statler, T. S., King, I. R., Crane, P., et al. 1999, AJ, 00, in press
- Tremaine, S. 1995, AJ, 110, 628
- Tsuboi, M., Miyazaki, A., & Tsutsumi, T. 1999, in Galactic Center Workshop 98: The Central Parsecs ([000 : 000]), in press
- van Bueren, H. G. 1978, A&A, 70, 707
- van Langevelde, H. J., Frail, D. A., Cordes, J. M., et al. 1992, ApJ, 396, 686
- Wouterloot, J. G. A. & Dekker, E. 1979, A&A Suppl., 36, 323
- Wright, M. C. H. & Backer, D. C. 1993, ApJ, 417, 560
- Yusef-Zadeh, F., Cotton, W., Wardle, M., et al. 1994, ApJ, 434, 63
- Yusef-Zadeh, F., Morris, M., & Chance, D. 1984, Nature, 310, 557
- Zhao, J.-H., Goss, W. M., Lo, K. Y., et al. 1991, ASP-CS, 31, 295

Table 1. Source Positions (B1950)

Source	RA h m s	DEC d m s	4.9-GHz Flux Jy	8.4-GHz Flux Jy
B1741-038	17 41 20.616	-03 48 48.90	2.09	1.75
B1748-253	17 48 45.792	-25 23 17.74	0.507	0.289
Sgr A*	17 42 29.319	-28 59 18.54	0.652	0.620
GC441	17 37 43.1110	-29 28 20.000	0.035	0.018
offset	-0.0107	+0.057		
B1737-294	17 37 43.1003	-29 28 19.943		
W56	17 42 42.7670	-28 19 17.700	0.105	0.112
offset	-0.0106	+0.037		
B1742-283	17 42 42.7564	-28 19 17.663		
W109	17 45 34.7400	-29 06 43.400	0.071	0.072
offset	-0.0049	+0.002		
B1745-291	17 45 34.7351	-29 06 43.398		

Table 2. FK5 Source Positions (J2000)

Source	RA h m s	DEC d ' "
J1751-2524 (B1748-253) ^a	17 51 51.2632	-25 24 00.062
1743-0350 (B1741-038) ^a	17 41 58.8561	-03 50 04.617
J1745-2900 (Sgr A*) ^{b,c}	17 45 40.0385	-29 00 28.104
J1740-2929 (B1737-294) ^c	17 40 54.5249	-29 29 50.290
J1745-2820 (B1742-283) ^c	17 45 52.4949	-28 20 26.270
J1748-2907 (B1745-291) ^c	17 48 45.6841	-29 07 39.374

^aFrom VLA CAL Manual, <http://www.nrao.edu/~gtaylor/csource.html#17>

^bCoordinates are for proper motion epoch 1998.3

^cestimated 1σ accuracy is 0.005"

Table 3. Observation Block Typical Schedule

Source	Start	Stop
1741-038	09:47:00	09:49:20
1748-253	09:51:30	09:53:20
GC441	09:54:50	09:57:50
W56	09:58:20	19:01:20
W109	10:01:50	10:04:50
SGRACN	10:05:30	10:07:50
GC441	10:08:30	10:11:20
W56	10:11:50	10:14:50
SGRACN	10:15:30	10:17:50
W109	10:18:30	10:21:20
GC441	10:21:50	10:24:40
SGRACN	10:25:20	10:27:40
W56	10:28:20	10:31:10
W109	10:31:40	10:34:40
SGRACN	10:35:20	10:37:40
GC441	10:38:20	10:41:10
W56	10:41:40	10:44:40
W109	10:45:10	10:48:10
1748-253	10:48:50	10:52:10
1741-038	10:59:20	11:02:10

Table 4. Journal of Observations

Epoch	Day	Date	JD	band	VLA Tape	Files	Code
1	1	81mar04	2444667.5	CCCCC	XL81003	33,34	BACK
1	2	81mar05	2444668.5	CCCCC	XL81003	36,37	BACK
2	1	82apr25	2445084.5	CCCCC	XH82007	45,46	BACK
2	2	82apr26	2445085.5	CCCCC	XH82007	48,49	BACK
2	3	82apr27	2445086.5	CCCCC	XH82008	3,4	BACK
3	1	83sep02	2445579.5	CCCCC	XH83016	24,25,26	AB248
3	2	83sep09	2445586.5	CCCCC	XH83017	7,8	AB248
3	3	83sep16	2445593.5	CCCCC	XH83017	40,41	AB248
4	1	85jan05	2446070.5	CCCCC	XH85001	18,19	AB248
4	2	85jan19	2446084.5	CCCCC	XH85003	7,8,9	AB248
4	3	85jan29	2446094.5	CCCCC	XH85004	25,26	AB248
5	1	86apr17	2446537.5	CCCCC	XH86011	9,10,11	AB388
5	2	86apr29	2446549.5	CCCCC	XH86012	24,25,26	AB388
5	3	86may29	2446579.5	CCCCC	XH86016	3,4,5	AB388
6	1	89jan28	2447554.5	CCCXC	XH89003	14	AB520
6	2	89feb02	2447559.5	CCCXC	XH89004	10	AB520
6	3	89feb04	2447561.5	CCCXC	XH89004	13,14	AB520
7	1	94apr02	2449444.5	CCXC	XH94024	8,9	AB708
7	2	94apr21	2449463.5	CCXC	XH94028	7,8	AB708
7	3	94apr26	2449468.5	CCXC	XH94029	3	AB708
8	1	98apr10	2450913.5	CCXC	XH98038	7	AB857
8	2	98apr18	2450921.5	CCXC	XH98040	9,10	AB857
8	3	98apr24	2450927.5	CCXC	XH98042	2	AB857

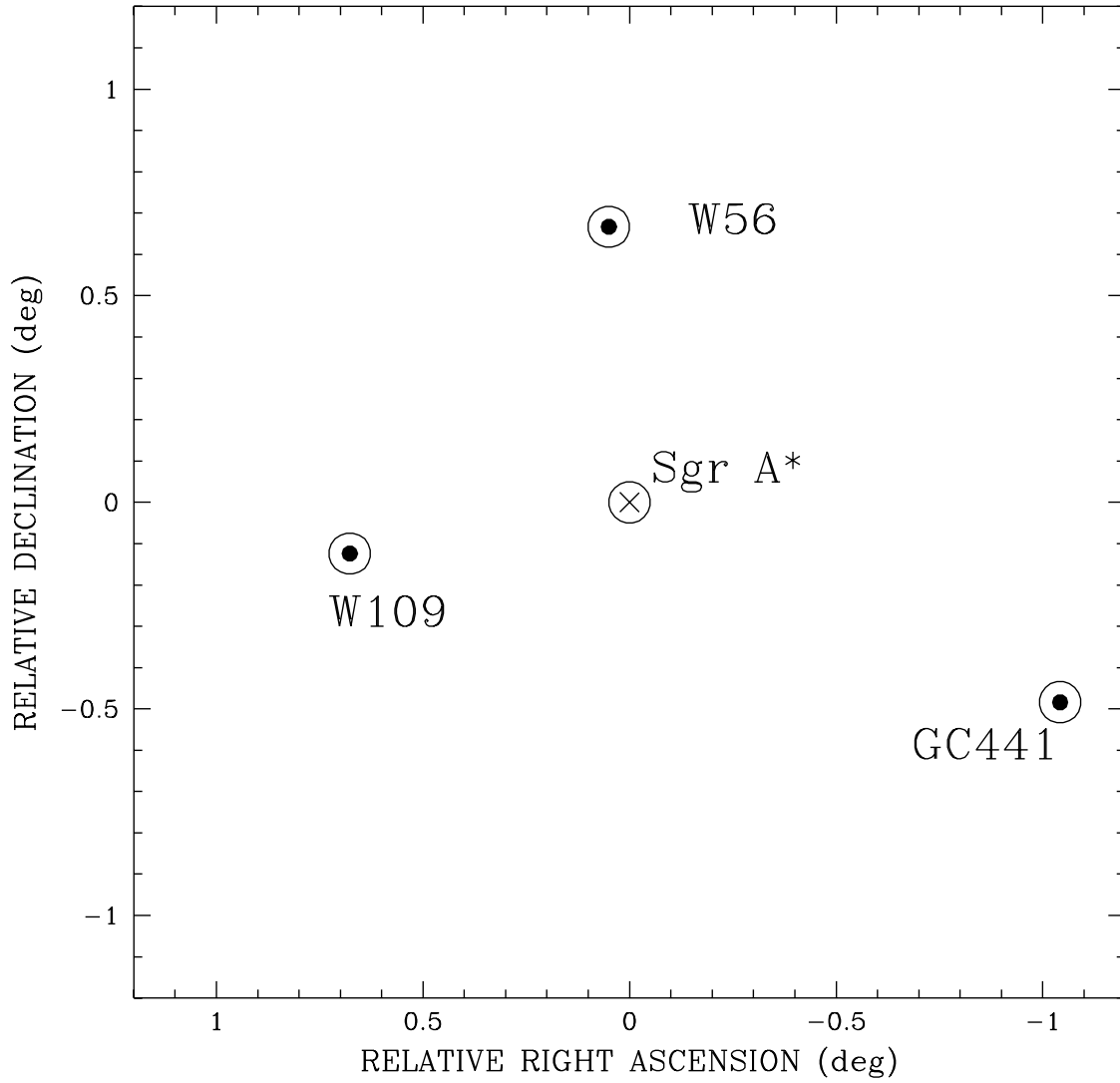


Fig. 1.— The relative locations of Sgr A* which is at origin and three reference sources, W109, W56 and GC441. Observations consisted of frequent switching between the reference sources and Sgr A*.

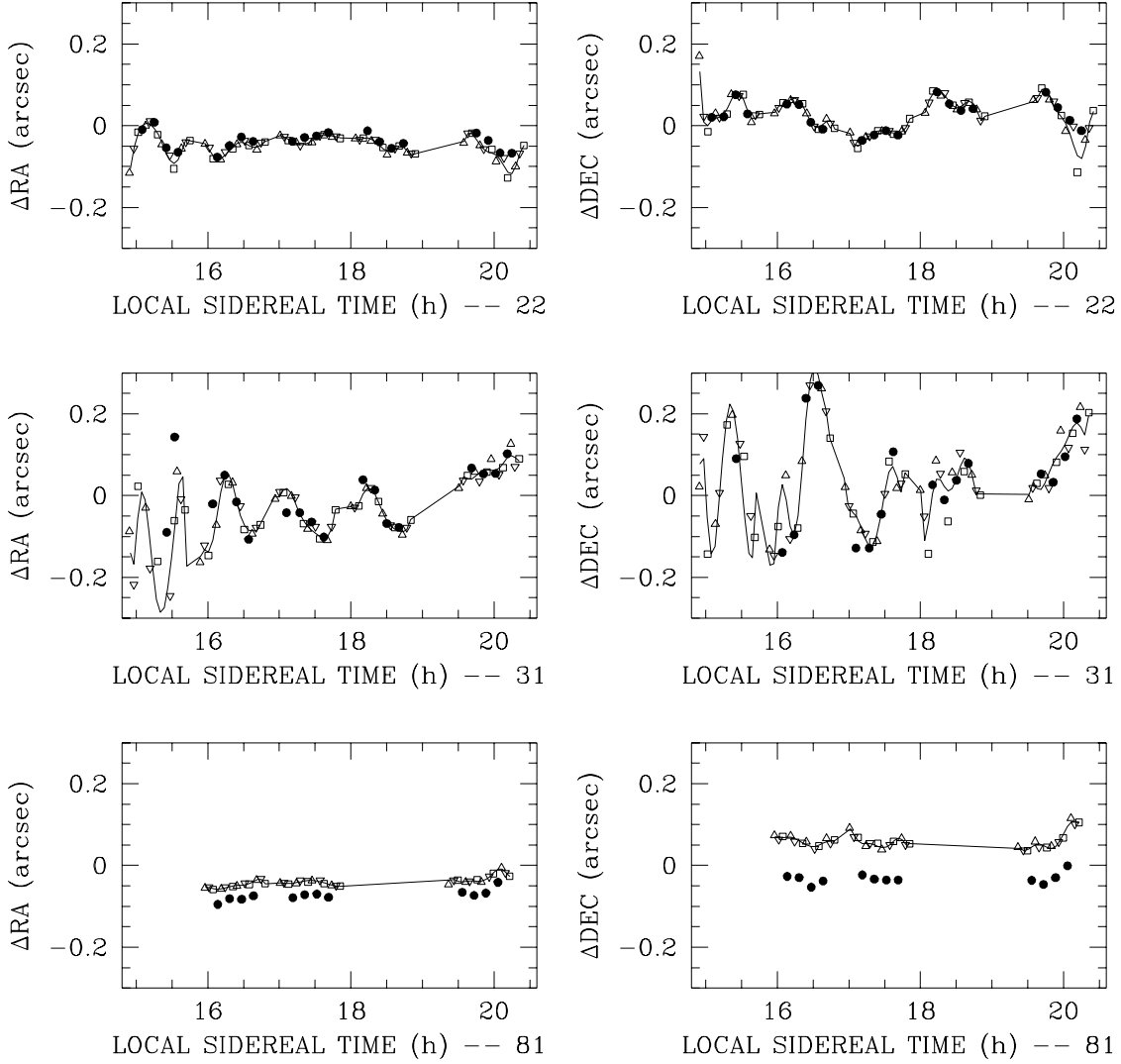


Fig. 2.— First difference positions (hourly phase calibration by B1748-253) in right ascension and declination for our three reference sources (open symbols: triangle=GC441; inverted triangle=W56; square=W109) and for Sgr A* (solid circular symbol) for three epochs. The solid line represents the 8th-order temporal polynomial fit to the reference source data. Abscissa axes provide the epoch keys: 22=epoch 2 day 2; 31=epoch 3 day 1 (a ‘bad’ day on the Plains of St. Augustin); and 81=epoch 8 day 1 (a ‘spectacular’ day).

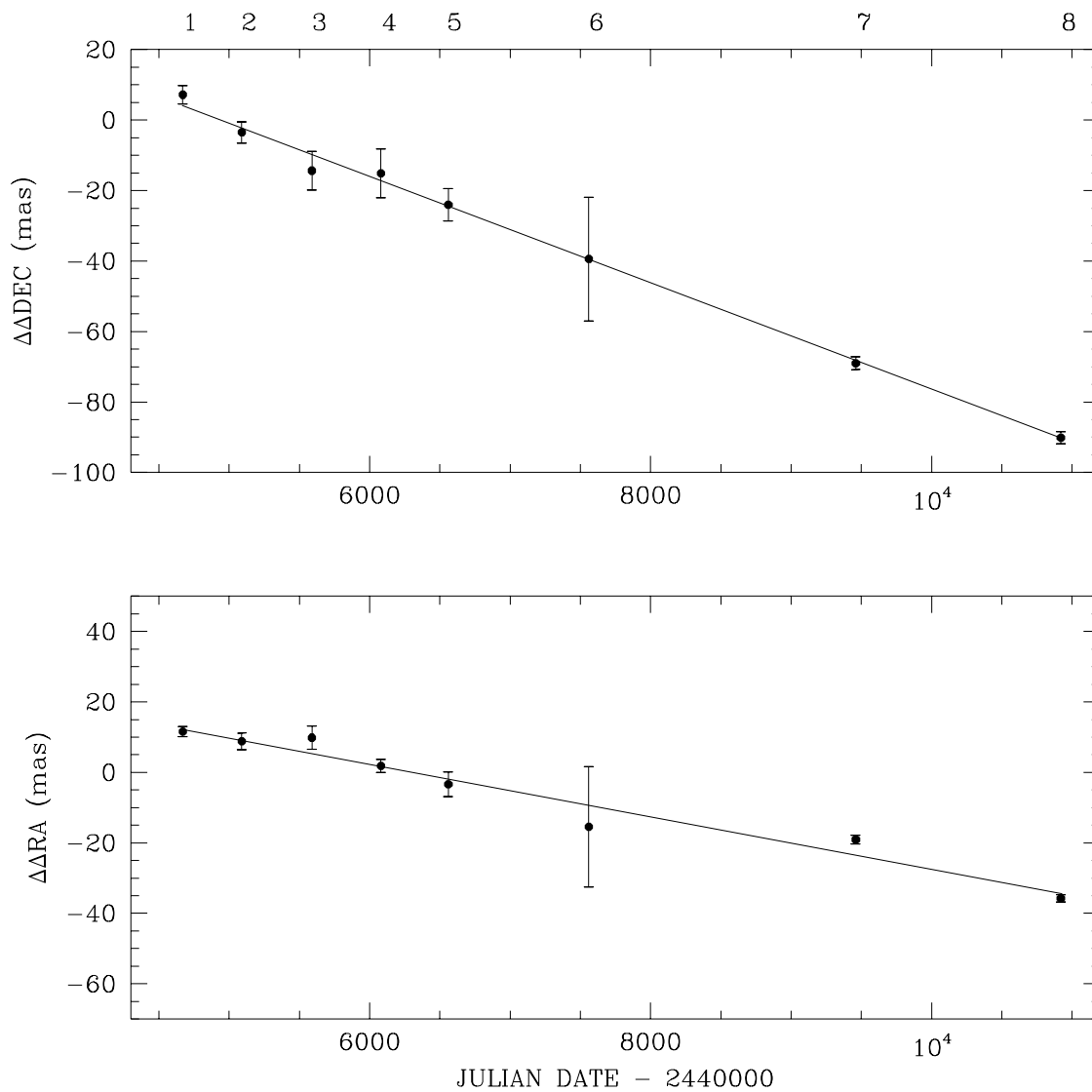


Fig. 3.— Weighted average second difference positions in right ascension and declination for Sgr A* using LST blocks at 16, 17, and 19 hours from VLA observations at 4.9 GHz. Errors are derived from the internal rms assuming independence of results in different blocks and on different days. Typically 9 measurements are included. The solid line gives best fit proper motion for Sgr A*. Epochs are enumerated at top.

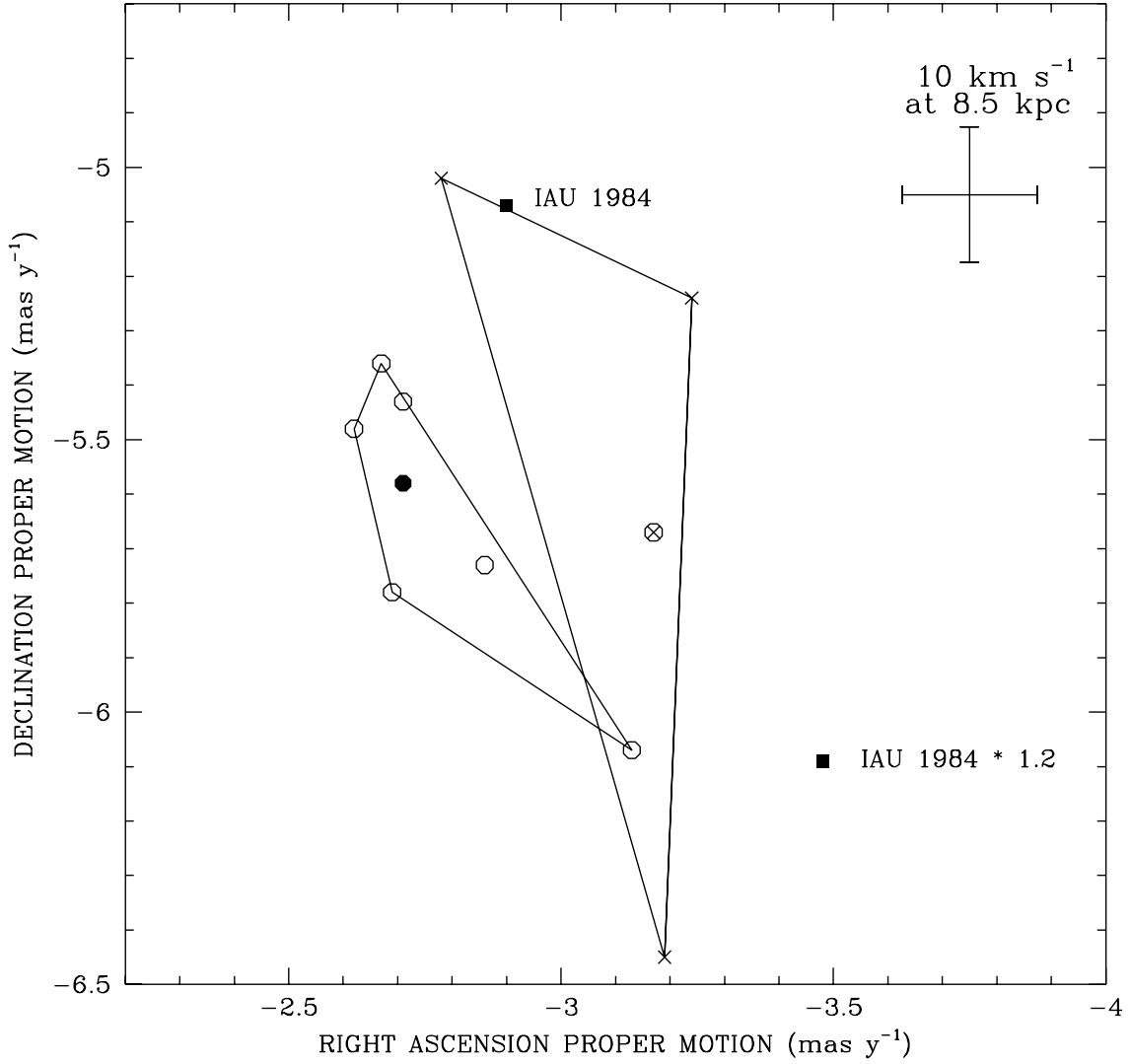


Fig. 4.— Proper motion estimates. Circular symbols points are based on 8 epochs (16 y) of 5-GHz data. The solid circle is from a weighted fit to all data. The open circles are from subsets of the data: each of 3 hour-long blocks and each of three days for 5 GHz. The X symbol points are from three epochs (9 y) of 8.4-GHz data. The circled- X is from a weighted fit to all data. The plain X are from each of three days. The spread in these subset points provides our best estimate of the errors quoted in the text for these two measurements. The solid square symbol points give the expected proper motion components for an object at rest in the galactic center owing to reflex motion of galactic rotation and solar motion with respect to local standard of rest. That labeled IAU 1984 uses Oort’s constants (A-B) in angular units given by the 1984 IAU value ($220 \text{ km s}^{-1} / 8.5 \text{ kpc}$) summed with the solar motion. The second point labeled IAU 1984 $\times 1.2$ is the result with (A-B) increased by 20%.

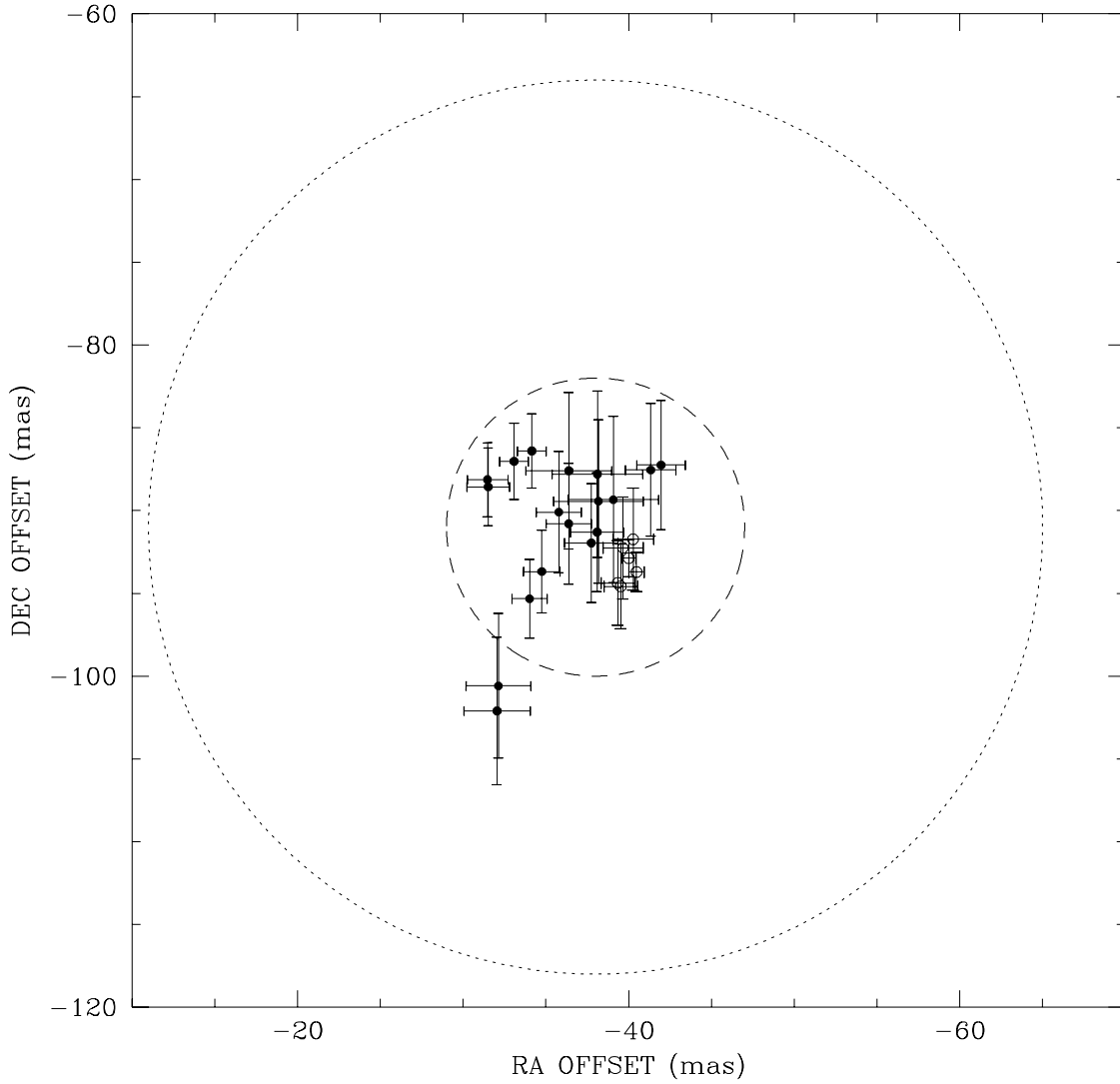


Fig. 5.— Second difference positions for Sgr A* from VLA observations at 4.9 GHz (closed symbol) and 8.4 GHz (open symbol) during epoch 8 when ‘radio seeing’ conditions were superb. Each point represents an average over a single 1-hour block of observations on a single day. Both VLA IFs are processed and the very high correlation of pairs of points is obvious. The two circles represent the diameters of the scatter broadened images at the two frequencies.

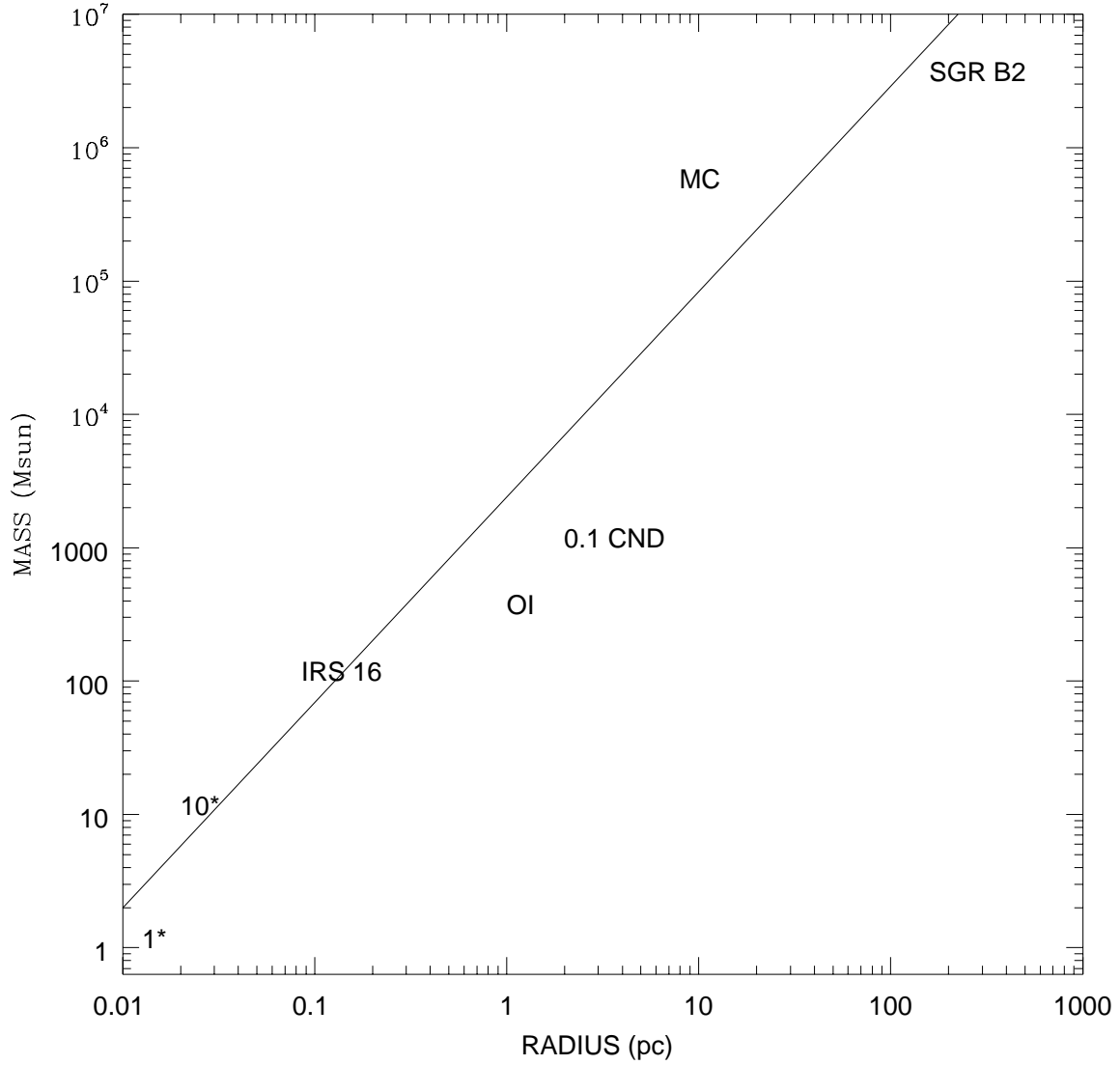


Fig. 6.— Asymmetric masses near the center of the galaxy as a function of distance from Sgr A* that will affect the location and motion of the barycenter of the galaxy. The line plotted has a slope of 1.5, $M(r) = 1000r^{1.5}$ where M is in solar mass units and r is in parsecs.